Validation of Proposed Integrated EEG/MEG and fMRI Model Using Real Data

Abbas Babajani-Feremi, John E. Moran, and Hamid Soltanian-Zadeh, *Senior Memner, IEEE*

***Abstract*—Main objective of this paper is to present methods and results for estimation of parameters of our proposed integrated magnetoencephalography (MEG) and functional Magnetic Resonance Imaging (fMRI) model. We use real auditory common MEG and fMRI datasets from 7 normal subjects to estimate the parameters of the model. The MEG and fMRI data was gathered at different times but the stimulus profile was the same for both techniques. We use independent component analysis (ICA) to extract temporal information from the MEG data. The stimulus correlated ICA component is used to estimate MEG parameters of the model. The temporal and spatial information of the fMRI datasets are used to estimate fMRI parameters of the model. Goodness of fit of the real data to our model confirms ability of the proposed model to simulate realistic datasets for evaluation of integrated fMRI/MEG analysis methods. It also makes it possible to use the proposed model in real applications.**

I. Introduction

MAGNETOENCEPHALOGRAPHY (MEG) and functional Magnetic Resonance Imaging (fMRI) have complementary spatial and temporal resolutions. fMRI has good spatial resolution but poor temporal resolution due to the limited rate of change in the hemodynamic response. On the other hand, MEG has good temporal resolution but its spatial resolution is poor due to ill-posedness of the inverse solution [1]. Integrated MEG/fMRI analysis should improve the overall spatiotemporal resolution of the results based on the fact that MEG and fMRI are different views of a common source (neural activity) [2-7].

Although MEG and fMRI signals originate from common sources (neural activities), there may be differences between the spatiotemporal responses of the two techniques [8]. An integrated bottom-up model based on physiological principles can illustrate the relationship between MEG and fMRI. However, there are limited works about MEG, electroencephalography (EEG), and fMRI integrated modeling in the literature [9-14].

Manuscript received September 28, 2007. This work was supported by grants from the University of Tehran, Tehran, Iran, and National Institutes of Health (NIH R01EB002450), United States.

A. Babajani-Feremi is with the Image Analysis Lab., Radiology Department, Henry Ford Hospital, Detroit, MI 48202, USA. (phone: 001-313-874-4360; fax: 001-313-874-4494; e-mail: abbasb@ rad.hfh.edu).

J. H. Moran, is with the Neuromagnetism Lab., Neurology Department, Henry Ford Hospital, Detroit, MI 48202, USA.

H. Soltanian-Zadeh is with the Image Analysis Lab., Radiology Department, Henry Ford Hospital, Detroit, MI 48202, USA and Control and Intelligent Processing Center of Excellence, Electrical and Computer Engineering Department, University of Tehran, Tehran 14395-515, Iran.

In the integrated model proposed in [11], a two-dimensional autoregressive model with exogenous variables (ARx) was introduced to describe the relationships between synaptic activity and homodynamic response. A static nonlinear function was used to describe the electro-vascular coupling through a flow-inducing signal. Their assumption about linear relationship between cerebral blood flow (CBF) and Blood Oxygen Level Dependent (BOLD) is not generally valid [15] which they correct it in [12] using the extended Balloon model (EBM) [16].

We proposed an integrated MEG/fMRI model [9] where post synaptic potentials (PSPs) were the main link between the MEG and fMRI (Fig. 1). For a given external stimulus in this model, a linear model represents the number of active PSPs at each time. Several parameters of PSPs were introduced and modeled using random variables. Different aspects of PSPs were considered for constructing the equivalent current dipole (ECD) and the overall synaptic activities in MEG and fMRI parts of the model, respectively. The MEG signal was constructed using the resultant ECD and solution of the forward problem. The fMRI signal was constructed using the resultant overall synaptic activities as the input of the EBM. Using simulation studies, we showed that the parameters of the model can explain conditions for which there is a detectable fMRI signal in an area but this area is silent for MEG and vice versa.

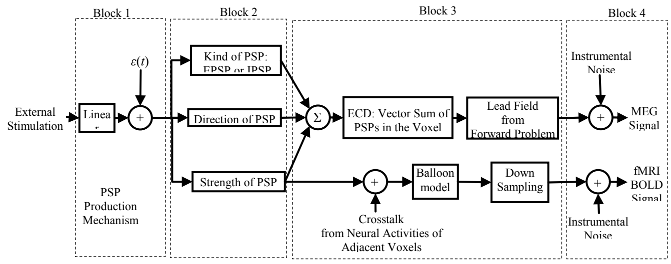

Fig. 1. Schematic Diagram for the proposed integrated MEG and fMRI model.

Using our proposed extended neural mass (ENM) model, we introduced other integrated model [10] based on the physiological principles of the cortical minicolumns and their connections. In this model, MEG signals are generated by synaptic activations of the pyramidal cells and sub-sequential currents in minicolumns that have been collectively modeled as an equivalent current dipole (ECD). By introducing a relationship between the stimulus and the overall neural activity and using it as the input of the EBM, we extracted the fMRI signal from the proposed extended neural mass model. We validated the proposed model by experimental results.

The main aim of the current paper is to determine the parameters of our proposed model [8] using MEG and fMRI data recordings of cortical responses to an auditory stimulus. While it was impossible to record MEG and fMRI signals simultaneously, these data were gathered from 7 normal subjects using the same on/off stimulus block design. Each block consisted of 12 seconds of “tones on” followed by 12 seconds of “tones off” (Fig. 2). After calculating the average MEG block response, we used independent component analysis (ICA) to extract the MEG signal of brain activity occurring in the primary auditory cortex. This signal was used to estimate parameters of the linear filter in Block 1 of Fig. 1. The corresponding spatio-temporal sequence of the fMRI activation, measured in the primary auditory cortex, was used to estimate the fMRI parameters of the proposed model. Goodness of fit of the real data with our model suggests that the proposed model is well suited for integrated fMRI/MEG analysis of the brain activity.

The organization of the paper is as follows. The summary of the proposed model in [9] is described in Section II. Description of the real auditory datasets and estimation of the parameters of the proposed model are presented in Section III. Conclusions are given in Section IV.

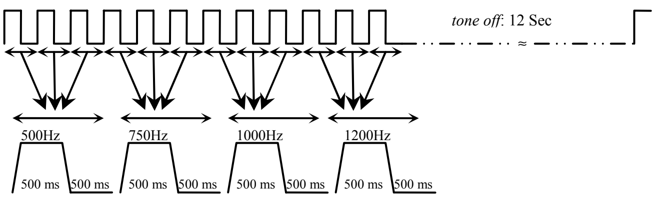

Fig. 2. Illustration of one epoch (block) of the stimulus profile for an auditory excitation. Each epoch contains 12 seconds of *tones on* and 12 second of *tones off* period. During the *tones on* period, 3 tone bursts were presented with a 15 ms rise/fall time at a rate of one per second for each of 4 tone frequencies 500Hz, 750 Hz, 1000 Hz, and 1200 Hz. MEG data of all subjects contained 50 epochs, but the number of fMRI blocks was different for different subjects (see Table 1).

II. Proposed Integrated Model

A. Introducing the Model

We proposed an integrated MEG/fMRI model in [9] whose main features are shown in Fig. 1. External stimulus causes neural activities in certain areas of the brain (activated regions). PSPs and action potentials (APs) are two main indices for neural activities. Based on several previous experimental results, it was concluded that both MEG and fMRI are mainly related to the PSPs and there is no noticeable correlation between these techniques and the APs. Thus, we assumed that the PSPs are the main link between the MEG and fMRI signals.

Relationship between the external stimulus and the number of active PSPs are shown in Block 1 of Fig. 1. We considered a linear system whose input is the external stimulus and its output is the number of active PSPs at each time point. While the relationship between the number of active PSPs and strength of the stimulus may be nonlinear, we assumed the following linear model for the sake of simplicity.

$$\sum_{k=0}^{r} a_k \frac{d^k N(t)}{dt^k} = N_{ss}\, Stm(t-\tau_{af}) \qquad (1)$$

where $N(t)$ is the number of active PSPs at time point t, a_k are coefficients of the linear system, and τ_{af} is the delay due to different relay processes in the long afferent pathways. For the block designs, $Stm(.)$ is the unit function and N_{ss} is the steady state value of $N(t)$. For the event related designs, $Stm(.)$ is the Dirac delta function and N_{ss}/a_1 is the peak value of $N(t)$.

Block 2 in Fig. 1 shows the relationship between the MEG and fMRI signals and the different aspects of the PSPs. There are some differences between the EPSP (excitatory PSP) and IPSP (inhibitory PSP) from the MEG point of view. The EPSP and IPSP can cancel each other in the MEG signal due to their opposite polarizations. In addition, the spatial locations and distributions of the excitatory and inhibitory synapses in a neuron are different as considered in the proposed model. We reviewed some experimental results about the difference of the EPSP and IPSP from the fMRI point of view. Our final conclusion was that there is almost no difference between EPSP and IPSP in consuming energy and thus there is no difference between them from the fMRI point of view in the proposed model. The direction of the current dipole produced by a PSP is important for the MEG signal, but does not have any effects on the fMRI signal. The strength of a PSP is important for both MEG and fMRI signals. We considered the above principles in extracting the MEG and fMRI signals from the active PSPs.

Since each active cortical area contains a huge number of neurons and synapses whose activities are not deterministically known, we considered stochastic models for the parameters (like direction, distribution, and strength) of the PSPs. A comprehensive description of the parameters and related probability density functions (pdf) of all parameters is presented in [8]. For producing MEG and fMRI signals for a given external stimulus, we first calculated the number of active PSPs ($N(t)$ in Eq. (1)). Then, the equivalent current dipole (ECD) and the overall neural activities were calculated. The MEG signal was extracted by considering solution of the forward problem and the resultant ECD in the active areas. The calculated overall neural activity was given as the input to the extended balloon model (EBM) [16] to generate the BOLD signal.

We considered spatial crosstalk in fMRI as shown in Fig. 1. The spatial crosstalk means that neural activities in a voxel change its blood flow and that of the neighboring voxels. Based on the existing experimental results about it, we formulated the spatial crosstalk with a Gaussian kernel [8].

B. Generating MEG and fMRI Signals by the Model

We extracted the MEG and fMRI signals from the external stimulus in the proposed integrated MEG/fMRI model [9]. The final results are briefly explained in this section. For extracting the MEG signal, we derived a relationship between the parameters of active PSPs and the generated ECD in the active area. The MEG signal was calculated using the resultant ECD and solution of the forward problem. In the fMRI part of the model, we introduced a relationship between the strength of the active PSPs in an active area and the overall synaptic activities. The overall resultant synaptic activities were used as the input of the EBM for producing the BOLD output.

Referring to Eq. (17) in [9], the mean ECD in an active area is:

$$\overline{Q}(t) = \overline{\varphi}\,\overline{V}\,\overline{\beta}\;[(1-r)\,g(\sigma_T^E) - r\,g(\sigma_T^I)].N(t) \tag{2}$$

where $\overline{\varphi}$ is a mean value related to the waveform of the PSPs, $\overline{V}$ is the mean amplitude of the PSPs, $\overline{\beta}$ is a mean value related to the parameters of dendrites, r is the ratio of the number of IPSPs to the number of all PSPs, and $g(\sigma_T^E)$ and $g(\sigma_T^I)$ are related to the spatial distributions of the EPSPs and IPSPs, respectively. $N(t)$ is the number of active PSPs at time point t according to Eq. (1). In a specific active cortical area, assuming known pdfs for all random variables, we have:

$$\overline{Q}(t) = K_M.N(t) \tag{3}$$

where K_M is a fixed parameter that represents the mean of all random variables in (2). The MEG signal is calculated using the ECD in (3) and the solution of the forward problem.

$$B(t) = G\,\overline{Q}(t) \tag{4}$$

where G is the lead field matrix and $B(t)$ is the measured field by the MEG sensors.

Referring to Eqs. (19) and (21) in [9], the overall synaptic activities due to the external stimulus is:

$$\begin{cases} \overline{u}(t) = K_f.N(t) \\ K_f = \dfrac{u_m}{\max(N)} \end{cases} \tag{5}$$

where $\overline{u}$ is the overall synaptic activities in the active cortical area, u_m is the synaptic activity that produces the maximum output in the extended Balloon model, max(N) shows the maximum number of active PSPs in the active area, and $N(t)$ represents the number of active PSPs according to (1). The calculated overall synaptic activity in (5) was used as the input of the EBM with the following equations:

$$\begin{cases} \ddot{f} = \varepsilon\overline{u}(t) - \dot{f}/\tau_s - (f-1)/\tau_f \\ \dot{v} = \dfrac{1}{\tau_0}(f - v^{1/\alpha}) \\ \dot{q} = \dfrac{1}{\tau_0}\left(f\,\dfrac{1-(1-E_0)^{\frac{1}{f}}}{E_0} - qv^{\frac{1}{\alpha-1}}\right) \\ y(t) = V_0(k_1(1-q) + k_2(1-q/v) + k_3(1-v)) \end{cases} \tag{6}$$

where the blood flow f, the blood venous volume v, and the veins deoxyhemoglobin content q are three state variables normalized to their rest values and y is the BOLD output signal. The neural efficiency (ε), the signal decay (τ_s), the autoregulation (τ_f), the venous transit time (τ_0), the stiffness (α), the oxygen extraction at rest (E_0), and the resting blood volume fraction (V_0) are the physiological parameters of the EBM. For a 1.5 T scanner and TE = 40 ms, parameters k_1, k_2, and k_3 have been evaluated to be $k_1 = 7E_0$, $k_2 = 2$, and $k_3 = 2E_0$-0.2 in [15]. We use $N(t)$ as $\overline{u}(t)$ in (6) and the effect of K_f in (5) is considered in ε.

III. Estimation of the Model Parameters

A. Auditory Task Data

One block of the auditory on/off stimulus is shown in Fig. 2. The first 12 seconds consists of *"tones on"* followed by 12 seconds of "*tones off*". During the *"tones on"* period, half second tone bursts with a 15 ms rise/fall time are presented at a rate of one per second. Three tone bursts are presented sequentially for each of 4 tone frequencies, in the following order, 500Hz, 750 Hz, 1000 Hz, and 1200 Hz. While it is impossible to gather MEG and fMRI data simultaneously, this auditory block stimulus is used for both MEG and fMRI studies of 7 healthy subjects (4 males and 3 females, from 27 to 44 years old). In addition, 3-D anatomical MRI data is used for co-registering fMRI and MEG coordinates. Specifications of the acquired MRI and fMRI data from the subjects are given in Table 1.

Table 1. Specification of the MRI and fMRI datasets used for estimating the parameters of the proposed model.

Subject #	Gender/ Age	MRI	fMRI			
		Resolution/ Voxel Size (mm^3)	Resolution/ Voxel Size (mm^3)	Volume Number	TR(s)/ TE (ms)	Number of Stimulus Block
1	Female/ 44	256x256x60/ 0.94x0.94x2.5	64x64x14/ 3.75x3.75x5.0	132	3/ 40	16.5
2	Female/ 40	256x256x60/ 0.94x0.94x2.5	64x64x16/ 3.75x3.75x5.0	198	2/ 30	16.5
3	Male/ 33	256x256x66/ 0.94x0.94x2.5	64x64x16/ 3.75x3.75x5.0	198	2/ 30	16.5
4*	Female/ 41	256x256x62/ 0.94x0.94x2.5	64x64x14/ 3.75x3.75x5.0	198	2/ 30	16.5
5*	Male/ 33	256x256x64/ 0.94x0.94x2.5	64x64x16/ 3.75x3.75x5.0	198	2/ 30	16.5
6	Male/ 27	256x256x154/ 0.94x0.94x1.0	64x64x34/ 3.44x3.44x3.5	120	2/30	10
7	Male/ 35	256x256x154/ 0.94x0.94x1.0	64x64x34/ 3.44x3.44x3.5	120	2/30	10

* Two fMRI Datasets are acquired.

For the fMRI data, we use a 1.5 T GE scanner and the echo planner imaging (EPI) sequence with 64 by 64 data acquisition matrix. Auditory stimuli are presented through air conductance tubes to headphones to reduce external noise. The MEG data is gathered by a 148 channel whole head Neuromagnetometer (4D Neuroimaging). Measurements are taken inside a magnetically shielded room located in the Neuromagnetism Laboratory of Henry Ford Hospital (HFH), Detroit, Michigan, USA. 50 blocks (epochs) of the MEG data are acquired for all subjects, sampled at 508.63 Hz, and initially band-pass filtered between 0.1-100 Hz before disk storage.

B. Preprocessing

One We use statistical parametric mapping (SPM) for activation detection of the fMRI data. After discarding first few slices, we do realignment and co-registration using SPM5. For finding the active voxels, the stimulus is convolved with three basis functions (HRF, HRF time derivative and HRF dispersion). A cluster of voxels above a statistical threshold is selected for each subject, focusing on primary auditory area. For each of the active voxel, the average BOLD signal over all blocks is calculated after removing DC offset and linear trend. In the next section, we use this average BOLD signal to estimate fMRI parameters in these voxels for all subjects. The detected activation of a representative subject co-registered to MRI is shown in Fig. 3.

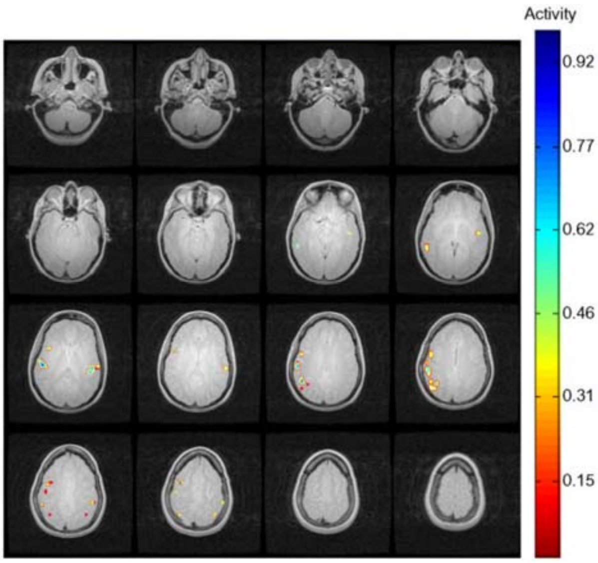

Fig. 3. Illustration of the detected activation from the fMRI data of subject # 2 co-registered to 3-D anatomical MRI data after removing single active voxels.

We use MEG-Tools (http://www.megimaging.com/) for coregistration of the MEG data with the 3-D anatomical MRI data. The MEG localizations are computed in reference to the Cartesian coordinate system defined by a set of three anatomical landmarks (fiducial points): the right and left external meatus or pre aurical and nasion. Prior to the MEG scan, the head surface is digitized using laser fast track scanning. The head digitization points (about 3,000 points) are used to ensure a precise registration, when the points laid on the scalp surface of the MRI scan.

The MEG data is band-pass filtered 0.5-30 Hz before analysis. The heart artifact is removed from the data. Bad epochs (blocks) containing eye blink are discarded and the remaining epochs are averaged to calculate the mean epoch data and improve the signal to noise ratio (SNR). We use ICA on the mean data as the final preprocessing stage after discarding the nuisance channels. Both “Fast-ICA” and AMUSE (Algorithm for Multiple Unknown Source Extraction) [17] algorithms are applied on the MEG datasets. We get higher SNR from AMUSE compared to “Fast- ICA”, confirming superiority of AMUSE as reported in [18].

The stimulus correlated component of ICA is called “ICA component” hereafter. ICA component for subject # 2 is illustrated in Fig. 4-a. The contour map of this component is shown in Fig. 4-b illustrating the existence of two ECDs in the left and right sides of the subject’s head corresponding to the activations within the primary auditory cortices.

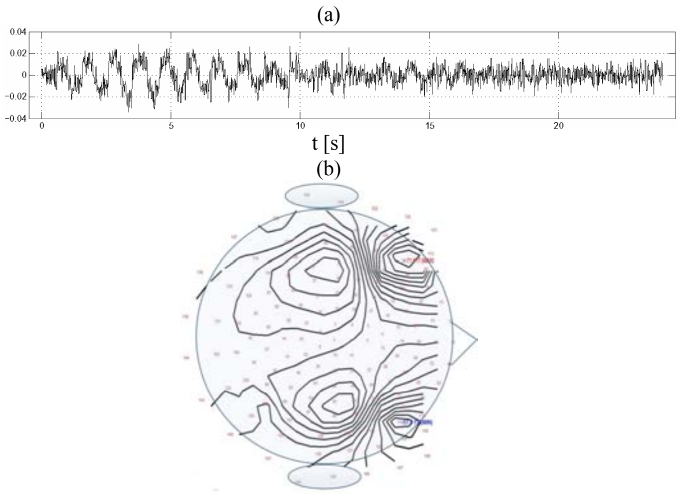

Fig. 4. Spatiotemporal illustration of the main ICA component of the MEG signal of subject # 2. (a) The ICA component correlated with the stimulus. (b) Contour map of this ICA component.

C. Parameter Estimation

After registering the MEG coordinates to the 3-D anatomical MRI data, the cortical model is constructed consisting of about 2,500 cortical locations in the subject’s gray matter. The concentric spherical head model is used to construct the forward model. We use the ICA component for activation detection in MEG. The correlation of this component with each sensor for subject # 2 is shown in the contour map of Fig. 4-b. The Multi-Resolution FOCUSS (MR-FOCUSS) [19] is used to solve the MEG inverse problem. The resulting activation for the ICA component of this subject is shown in Fig. 5. As illustrated in Figs. 3 and 5, the fMRI and MEG detect activations for subject #2 have appropriate spatial correlation. Also, the spatial overlap of the MEG and fMRI detected activations for other subjects are reasonable.

Considering the ICA component as the MEG signals on the sensors, we have:

$$B(t) = (b_1 \quad \dots \quad b_m)^T .IC(t) \tag{7}$$

where $IC(t)$ is the ICA component, $(b_1 \dots b_m)^T$ is an array showing correlation of m sensors with the ICA component, and $B(t)$ is the MEG signals on the sensors. Inverse solution of Eq. (4) using MR-FOCUSS gives $\hat{Q}(t) = G^+.B(t)$ where G^+ is the inverse kernel of G. Combining the inverse solution, Eq. (4), and Eq. (7), we have:

$$\hat{Q}(t) = [G^+(b_1 \quad \dots \quad b_m)^T].IC(t) \tag{8}$$

Comparing Eq. (3) with Eq. (8), it can be assumed that $\hat{N}(t) = IC(t)$ and $\hat{K}_M = G^+(b_1 \quad \dots \quad b_m)^T$. We calculate the ICA component for all of the subjects and consider it as $N(t)$ in Eq. (3). After solving the inverse problem and finding G^+, the estimated K_M in each voxel will yield the magnitude of the reconstructed dipole in that particular voxel.

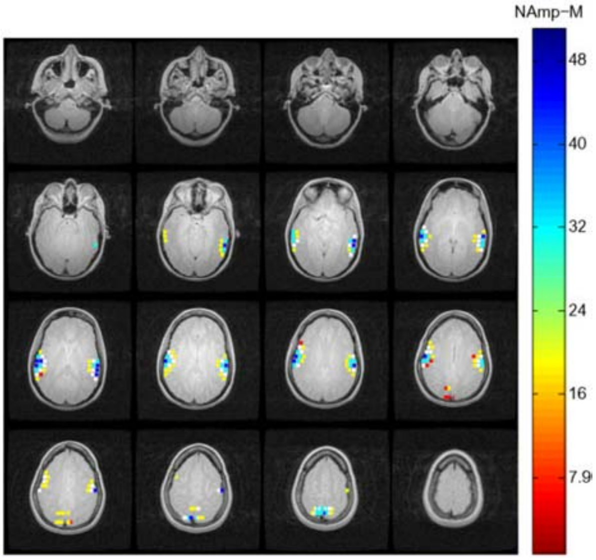

Fig. 5. MEG detected activations of subject #2 after co-registration to the 3-D anatomical MRI data.

After specifying $\hat{N}(t)$ as the ICA component, it is possible to estimate parameters of the linear filter in (1) with the given $\hat{N}(t)$ and the stimulus. For all subjects, we found that a first order linear filter generates reasonable estimation results. Thus, we use the following first order linear filter.

$$T_p \frac{dN(t)}{dt} + N(t) = K \, Stm(t - T_d) \tag{9}$$

where T_p , T_d , and K are parameters to be estimated. Considering noise, to estimate the parameters of the above linear filter, we have:

$$\begin{cases} N(t;\theta) = h(t;\theta) * Stm(t) \\ \hat{N}(t) = N(t;\theta) + e(t) \end{cases} \tag{10}$$

where $e(t)$ models the physiological and instrumental noises, $\hat{N}(t)$ is the calculated ICA component from the MEG data, and $h(t;\theta)$ is the impulse response of the linear filter in Eq. (9) with parameters θ=(T_p , T_d , K). If the noise model is Gaussian ($e \sim N(0,\Sigma)$), the parameters can be estimated by the maximum likelihood (ML) method as follows.

$$\begin{aligned} \hat{\theta}_{ML} &= \arg\max_\theta f(\hat{N};\theta) \\ &= \arg\min_\theta(-\log[f(\hat{N};\theta)]) \\ &= \arg\min_\theta \frac{[\hat{N}(t) - N(t;\theta)]^T \Sigma^{-1} [\hat{N}(t) - N(t;\theta)]}{2}. \end{aligned}$$

where $f(.)$ is the probability density function. Finding θ with ML method leads to weighted least square method with weight matrix Σ. Under the white noise assumption ($\Sigma = \sigma^2 I$), it leads to minimize the following least square function:

$$E(\theta) = \sum_t [\hat{N}(t) - N(t;\theta)]^2 \tag{11}$$

We use the numerical minimization method proposed in [20] for estimating θ=(T_p , T_d , K) where a quasi-Newton method using values of $E(\theta)$ as well as its gradient is employed. This method is implemented in Matlab with the function "*pem*". The $N(t)$ and $\hat{N}(t)$ for all subjects are illustrated in Fig. 6. The estimated values of θ=(T_p , T_d , K) for all subjects are given in Table 2. Signal to noise ratio related to the estimation of the linear filter in MEG (SNR_M) in this table is defined as $SNR_M = \|\hat{N}(t)\| / \|\hat{N}(t) - N(t)\|$. As illustrated in Fig. 6 and values of SNR_M in Table 2, the MEG data of some of the subjects have low SNR_M and thus the standard deviation (STDV) of the estimated parameters are a little high. We try to increase SNR_M and decrease STDV of the estimated values using higher order linear filters, but it did not generate much improvement.

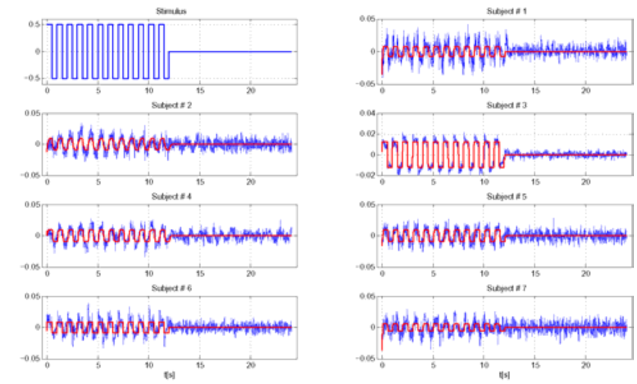

Fig. 6. Illustration of the estimated output of the linear filter in Eq. (9) and real MEG signals. Top-left subplot shows the stimulus as input of Eq. (9). Other subplots show estimated $N(t)$ (red plot) as output of Eq. (9) and real signal (blue plot) as main ICA component from MEG data.

For estimating the parameters related to the fMRI part of the model, we use estimation of θ=(T_p , T_d , K) and calculate the estimated $N(t)$ according to (9). Then, the estimated $N(t)$ assumed as overall synaptic activities $\bar{u}(t)$ in (5) to generate the estimated BOLD response in each active voxel. Parameters of the EBM are estimated by minimizing the error between the estimated and real fMRI signals. The measured BOLD signal can be modeled as follows.

$$y = g(\bar{u};\eta) + e, \qquad e \sim N(0,\Sigma) \tag{12}$$

where $g(\bar{u};\eta)$ is the output of the dynamical system of the EBM with input $\bar{u}$ (overall synaptic activities) according to (6), η=(ε, τ_s, τ_f, τ_0, α, E_0, V_0) is physiological parameters of the EBM, and e is the Gaussian measurement noise with variance Σ. If the nonlinear effects of the EBM are small enough, then the effect of physiological noise could be approximated as additive Gaussian noise and e in (12) could model both measurement and physiological noises [21]. Using similar steps to derive Eq. (11), the ML estimation of the parameter η leads to the following least square estimation assuming white Gaussian noise ($\Sigma=\sigma^2 I$):

$$\hat{\eta}_{LS} = \arg\min_{\eta} \sum_t [g(\bar{u}(t);\eta) - y(t)]^2 \qquad (13)$$

As described in Section III.B, the active voxels for each subject are chosen and their mean BOLD signal over all blocks are calculated and assumed as $y(t)$ in (13). Then, parameters of the EBM are estimated using a numerical minimization method. A basic question about the identifiability of the EBM is that if we know the system input $\bar{u}$ and output y, do we have enough information to determine unique values for the parameters? Although answer to this question in general case is hard, some insight can be inferred in specific cases. For example, if the input is low enough to make the linear approximation of the model, then the scale factor on the input (ε) and that on the output (V_0) have similar effects on the output. Indeed, increasing ε could be compensated by decreasing V_0 to produce the same output. Thus, it is not be possible to estimate these 2 parameters by having the input u and output y. More discussion about this question is found in [21]. For reducing the redundancy, we fix α=0.33, E_0=0.34, and V_0 = 0.03 (V_0 = 0.06 for subject # 6) at their physiological mean values according to [16] and estimate the remaining parameters η = (ε, τ_s, τ_f, τ_0).

For estimating the parameters of the EBM, we use "*Simulink*" toolbox and "*fminsearch*" function of the Matlab as shown in Fig. 7. First, the parameters of the linear filter in Eq. (9) are estimated using the MEG data and the estimated $N(t)$ is considered as the overall synaptic activity ($\bar{u}(t)$ in Eq. (6)). Then, the estimation process for the remaining parameters is started by choosing proper initial values. The "*fminsearch*" function, which uses the simplex search method, minimizes the sum square error between the real and estimated BOLD signals by iteratively changing the parameters of the EBM. "*Simulink*" is used to solve the nonlinear state-space equation (6) by the iterations of the "*fminsearch*" minimization.

The estimated parameters of the EBM for all subjects are given in Table 2. For each subject, the value of the parameter in this table is the mean of the estimated parameter in all active voxels. The histograms of 4 estimated parameters of the EBM for all subjects are illustrated in Fig. 8. We use principal component analysis (PCA) to extract the main component of the BOLD signal from all active voxels in each subject. Then, we estimate parameters of the EBM for this component. The estimated and the real BOLD signals for this PCA component of all subjects are shown in Fig. 9.

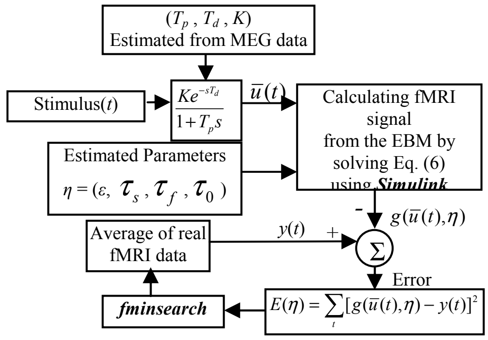

Fig. 7. Using "*fminsearch*" function and "*Simulink*" toolbox of Matlab for estimating parameters of the EBM. The parameters of the linear filter in Eq. (9) are estimated using MEG data and the output $N(t)$ is given as $\bar{u}(t)$ in Eq. (6). The "*fminsearch"* function minimizes the sum square error between the real and estimated BOLD signals by iteratively changing the parameters of the EBM. "*Simulink*" is used to solve the nonlinear state-space equation (6).

Subject # 6 has most BOLD contrast compared to others as shown in Fig. 9. When we fix V_0 = 0.03 for this subject, we find that the estimation process becomes unstable. Stable estimation needs higher value for V_0 according to the linear relationship between the BOLD contrast and V_0. Although "*fminsearch*" function tries to compensate the effect of V_0 by a large value for ε but it cannot be compensated due to the nonlinearity effect in the large input signal. We fix V_0 = 0.06 for this subject and get stable estimation. However, value of ε is still large for this subject as shown in Table 2. Subject # 7 also has high BOLD contrast and its estimated ε has a large value. Therefore, the distribution of the values for ε over the wide range shown in Fig. 8 is related to this fact that we fix V_0 and try to model its effect by ε.

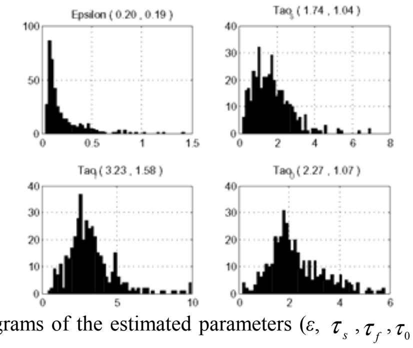

Fig. 8. Histograms of the estimated parameters (ε, τ_s, τ_f, τ_0) of the EBM for all subjects. α=0.33, E_0=0.34, and V_0 = 0.03 (V_0 = 0.06 for subject # 6) were fixed at their physiological mean values. Left and right values in parentheses of each subplot show the mean and the standard deviation of the estimated parameters, respectively.

The BOLD contrast of some subjects has low SNR as shown in Fig. 9 and Table 2. There are outliers in their real fMRI data. As "*fminsearch*" may find any minimum of Eq. (13), outliers can cause finding a local minimum instead of the global minimum. However, using norm one instead of norm two in (13) can reduce the effect of outliers. Thus, we repeat the estimation of the parameters using norm one.

However, mean values of the estimated parameters of the active voxels do not change significantly compared to the results from norm two given in Table 2.

Table 2. Estimated values of the parameters of the proposed integrated model using real auditory data of 7 normal subjects. The parameter T_p , T_d , and K are related to the linear filter in Eq. (9). MEG linear filter signal to noise ratio (SNR_M) is defined as $SNR_M = \|\hat{N}(t)\| / \|\hat{N}(t) - N(t)\|$ where $\hat{N}(t)$ is the estimate of $N(t)$ according to (9). Values under columns ε, τ_s , τ_f, and τ_0 are the mean value of these estimated parameters from all active voxels of the corresponding subjects. Mean and STDV rows show the average and the standard deviation of the estimated parameters for all subjects, respectively. fMRI Signal to noise ratio (SNR_f) is defined as $SNR_f = \|\hat{y}(t)\| / \|\hat{y}(t) - y(t)\|$ where $\hat{y}(t)$ and $y(t)$ are estimated and real BOLD signals, respectively. α=0.33, E_0=0.34, and V_0 = 0.03 (V_0 = 0.06 for subject # 6) were fixed at their physiological mean values.

	Parameters of the Linear Filter				Parameters related to Extended Balloon Model in fMRI						
Subject #	K_p	T_p (ms)	T_d (ms)	SNR_M	Active Voxel no.	σ (mm)	ε	τ_s (s)	τ_f (s)	τ_0 (s)	SNR_f
1	0.016	20	74	0.87	40	10.06	0.21	2.30	1.84	1.49	4.16
2	0.020	100	0	0.98	10	5.55	0.17	2.04	2.75	1.44	1.81
3	0.025	14	1	3.20	21	10.67	0.13	1.05	3.93	2.30	3.25
4	0.019	44	59	1.23	42	7.87	0.17	1.40	3.65	2.70	3.15
					28	10.11	0.16	1.40	4.23	2.30	3.54
5	0.020	31	72	1.40	82	8.01	0.17	1.93	3.44	2.82	3.03
					67	11.29	0.16	1.75	3.77	2.85	2.50
6	0.017	3	0	1.08	56	11.51	0.34	1.35	2.27	1.63	9.39
7	0.012	20	39	0.63	44	16.86	0.26	2.16	3.26	1.68	6.51
Mean	0.018	33	35	-	-	10.21	0.20	1.74	3.23	2.27	-
STDV	0.004	32	34			3.15	0.19	1.04	1.58	1.07	

The estimated values of the parameters of the EBM shown in Table 2 are in agreement with other works [16, 21]. Reasonable mean and STDV of the estimation are due to this fact that all datasets are from the normal subjects with the same stimulus. In addition, we have two series of fMRI datasets for subjects #4 and #5 whose estimated parameters are similar as shown in Table 2. Finally, Figs. 6 and 9 illustrate the goodness of fit of the real MEG and fMRI datasets to the proposed integrated MEG/fMRI model.

As the final stage, we estimate the parameter related to the spatial crosstalk in fMRI. Fig. 3 illustrates the detected activation from the fMRI time series of subject # 2 after removing the single active voxels. For estimating the spatial crosstalk represented by $\sigma = (\sigma_x, \sigma_y, \sigma_z)$ in Eq. (2) of [8], a Gaussian kernel is fitted to the main cluster of the detected activation area. We assume an isotropic Gaussian kernel with $\sigma_x = \sigma_y = \sigma_z$ for estimating σ_x, σ_y, and σ_z. The hotspot of the cluster is assumed as the center of the Gaussian kernel. All neighboring voxels to the central voxel in a sphere with a diameter of 25 mm are considered for curve fitting. The estimated σ is given in Table 2.

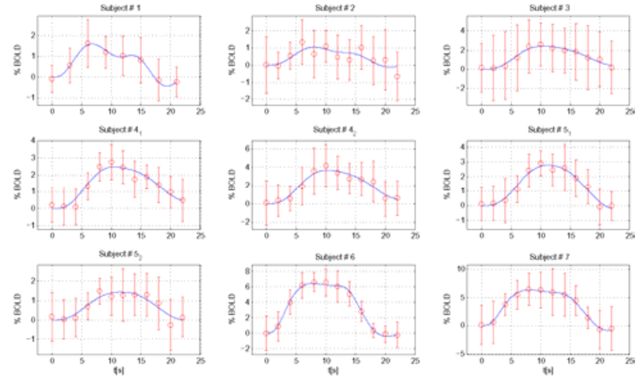

Fig. 9. Illustration of the real and the estimated BOLD signals. Red plots show the PCA main component extracted from the real data of all active voxels in each subject. This PCA component is the average of all blocks; o-plot and error-bar show the mean and the STDV of BOLD signals, respectively. The estimated BOLD signals are illustrated by blue lines. 2 series of fMRI data for subjects # 4 and #5 were used as specified by subscripts 1 and 2 in title of the corresponding subplots.

IV. Conclusion

In this paper, we estimate the parameters of the integrated MEG/fMRI model (Fig. 1) proposed in our previous work [8] using real data. In the proposed model, the external stimulus generates neural activities related to the PSPs which are the common link between MEG and fMRI. We use a first order linear filter to calculate the number of active PSPs as a function of the external stimulus. We summarize the relationship between the number of active PSPs as an index of neural activity and ECD that generates the MEG signal. Moreover, we define the relationship between the number of active PSPs and the overall synaptic activity as input of the EBM for generating the fMRI signal. We estimate parameters of the proposed integrated model using real auditory data from 7 normal subjects. We start with an ICA analysis of the MEG signal and show that the ICA component can be assumed as the number of active PSPs. Parameters of the first order linear filter and parameters of the EBM are estimated using the real data. The Goodness of fit of the real data to our model suggests the ability of the proposed model in simulating realistic datasets for integrated fMRI/MEG analysis. The proposed model with the parameters estimated from real data will be useful in evaluating and comparing different analysis methods of MEG and fMRI. It is also instrumental in characterizing the upcoming methods for integrated analysis of MEG and fMRI.

References

[1] M. Hämäläinen, R. Hari, R. J. Ilmoniemi, J. Knuutila, and O. V. Lounasmaa, "Magnetoencephalography - theory, instrumentation and applications to noninvasive studies of the working human brain," *Rev Mod Phys,* vol. 65, pp. 413-497, 1993.

[2] A. M. Dale and E. Halgren, "Spatiotemporal mapping of brain activity by integration of multiple imaging modalities," *Curr Opin Neurobiol,* vol. 11, pp. 202-8, Apr 2001.

[3] A. M. Dale, A. K. Liu, B. R. Fischl, R. L. Buckner, J. W. Belliveau, J. D. Lewine, and E. Halgren, "Dynamic statistical parametric mapping: combining fMRI and MEG for high-resolution imaging of cortical activity," *Neuron,* vol. 26, pp. 55-67, Apr 2000.
[4] B. Horwitz and D. Poeppel, "How can EEG/MEG and fMRI/PET data be combined?," *Hum Brain Mapp,* vol. 17, pp. 1-3, Sep 2002.
[5] A. K. Liu, J. W. Belliveau, and A. M. Dale, "Spatiotemporal imaging of human brain activity using functional MRI constrained magnetoencephalography data: Monte Carlo simulations," *Proc Natl Acad Sci U S A,* vol. 95, pp. 8945-50, Jul 21 1998.
[6] Z. Liu, L. Ding, and B. He, "Integration of EEG/MEG with MRI and fMRI," *IEEE Eng Med Biol Mag,* vol. 25, pp. 46-53, Jul-Aug 2006.
[7] E. Martinez-Montes, P. A. Valdes-Sosa, F. Miwakeichi, R. I. Goldman, and M. S. Cohen, "Concurrent EEG/fMRI analysis by multiway Partial Least Squares," *Neuroimage,* vol. 22, pp. 1023-34, Jul 2004.
[8] P. L. Nunez and R. B. Silberstein, "On the relationship of synaptic activity to macroscopic measurements: does co-registration of EEG with fMRI make sense?," *Brain Topogr,* vol. 13, pp. 79-96, Winter 2000.
[9] A. Babajani, M. H. Nekooei, and H. Soltanian-Zadeh, "Integrated MEG and fMRI model: synthesis and analysis," *Brain Topogr,* vol. 18, pp. 101-13, Winter 2005.
[10] A. Babajani and H. Soltanian-Zadeh, "Integrated MEG/EEG and fMRI model based on neural masses," *IEEE Trans Biomed Eng,* vol. 53, pp. 1794-801, Sep 2006.
[11] J. Riera, E. Aubert, K. Iwata, R. Kawashima, X. Wan, and T. Ozaki, "Fusing EEG and fMRI based on a bottom-up model: inferring activation and effective connectivity in neural masses," *Philos Trans R Soc Lond B Biol Sci,* vol. 360, pp. 1025-41, May 29 2005.
[12] J. J. Riera, X. Wan, J. C. Jimenez, and R. Kawashima, "Nonlinear local electrovascular coupling. I: A theoretical model," *Hum Brain Mapp,* vol. 27, pp. 896-914, Nov 2006.
[13] J. J. Riera, J. C. Jimenez, X. Wan, R. Kawashima, and T. Ozaki, "Nonlinear local electrovascular coupling. II: From data to neuronal masses," *Hum Brain Mapp,* vol. 28, pp. 335-54, Apr 2007.
[14] J. Daunizeau, C. Grova, G. Marrelec, J. Mattout, S. Jbabdi, M. Pelegrini-Issac, J. M. Lina, and H. Benali, "Symmetrical event-related EEG/fMRI information fusion in a variational Bayesian framework," *Neuroimage,* vol. 36, pp. 69-87, May 15 2007.
[15] R. B. Buxton, E. C. Wong, and L. R. Frank, "Dynamics of blood flow and oxygenation changes during brain activation: the balloon model," *Magn Reson Med,* vol. 39, pp. 855-64, Jun 1998.
[16] K. J. Friston, A. Mechelli, R. Turner, and C. J. Price, "Nonlinear responses in fMRI: the Balloon model, Volterra kernels, and other hemodynamics," *Neuroimage,* vol. 12, pp. 466-77, Oct 2000.
[17] L. Tong, R. Liu, V. C. Soon, and Y. F. Huang, "Indeterminacy and identifiability of blind identification," *IEEE Trans. Circuits. Syst.,* vol. 38, pp. 499-509, 1991.
[18] J. E. Moran, C. L. Drake, and N. Tepley, "ICA methods for MEG imaging," *Neurol Clin Neurophysiol,* vol. 2004, p. 72, 2004.
[19] J. E. Moran, S. M. Bowyer, and N. Tepley, "Multi-Resolution FOCUSS: a source imaging technique applied to MEG data," *Brain Topogr,* vol. 18, pp. 1-17, Fall 2005.
[20] L. Ljung, *System identification : theory for the user*, 2nd ed. Upper Saddle River, NJ: Prentice Hall PTR, 1999.
[21] T. Deneux and O. Faugeras, "Using nonlinear models in fMRI data analysis: model selection and activation detection," *Neuroimage,* vol. 32, pp. 1669-89, Oct 1 2006.